28. PHYSICAL PROPERTIES OF EQUATORIAL PACIFIC SEDIMENTS[1]

R. H. Wilkens, Earth Resources Laboratory, Department of Earth, Atmospheric, and Planetary Sciences, Massachusetts Institute of Technology
and
T. Handyside, Department of Geology, University of Newcastle-upon-Tyne[2]

ABSTRACT

The relationships between acoustic velocity, bulk density, grain density, porosity, carbonate content, thermal conductivity, and electrical conductivity (formation factor) in sediments from a single equatorial Pacific site from DSDP Leg 85 are examined. Bulk density and porosity are controlled by both compaction and composition. Silica-rich sediments are less dense because of lower grain density values and the grain shapes, which tend to hold the sediment framework open. Velocity increases slowly and uniformly with depth in the unconsolidated sediments and then increases in both magnitude and variability as lithification increases in the lower levels of the section. Density (and thus composition) controls acoustic impedance in the unconsolidated sediments, and the degree of lithification controls acoustic impedance lower in the section. Thermal conductivity values are in general agreement with theoretical values when composition is taken into account. Thermal conductivity and formation factor show a high degree of correlation. A comparison of vertical and horizontal values of formation factor indicates that horizontal electrical paths in the sediment are systematically more conductive than vertical paths. Both depth-dependent and time-dependent (synchronous) changes can be seen in all sites when downhole data are plotted versus first depth and then age.

INTRODUCTION

Measurements of the physical properties of marine sediments in combination with other observations from DSDP boreholes reveal information that can lead to a better understanding of the processes of sedimentation and lithification in the deep ocean. The primary goal of Leg 85 of the Deep Sea Drilling Project was to recover undisturbed sections of equatorial Pacific sediments by using the hydraulic piston corer (HPC) in soft sediments and by rotary coring in the deeper, partially lithified sections. The drilling presented an opportunity to investigate various physical properties of these sediments in great detail and to combine these data with the results of other investigations, such as the reflection seismic data from the site surveys, the lithostratigraphic descriptions of the recovered core, and the general paleoceanographic history of the individual sites as revealed in studies of carbonate content and microfossil assemblages.

In the course of the cruise, several thousand measurements were made on recovered core. The techniques and measurements included the gamma ray attenuation porosity evaluator (GRAPE) determination of fine-scale variations in porosity (Boyce, 1976); the gravimetric determination of wet-bulk density, water content, and porosity (Boyce, 1976); the measurement of compressional wave acoustic velocity (Boyce, 1977); the needle probe measurement of thermal conductivity (Von Herzen and Maxwell, 1959); the four-probe measurement of electrical conductivity, which was used to yield the ratio of seawater to sediment electrical conductivity (formation factor; Manheim and Waterman, 1974); and the determination of sediment shear strength by using the Wykeham-Farrance vane shear apparatus (Boyce, 1977). A complete tabulation of the resulting measurements is presented in the appendix to this volume.

These properties are plotted versus depth in the site chapters. This chapter does not repeat the results but rather examines the relationships among the properties at a single location, Site 574. We chose the Site 574 data for two reasons: (1) the sediments from Site 574 covered wide ranges of depth (0 to 520 m), age (0 to 39 Ma), and carbonate content (5 to 95%), and (2) the data for all of the properties measured are highly reliable, unlike the data for the other sites, into which one or another of the measurement procedures may have introduced some error. The trends apparent at Site 574 are much the same as at the other sites. We have chosen not to consider either the GRAPE or the shear strength data in this chapter. The GRAPE results are in good agreement with the gravimetric determinations of porosity for the HPC cores, but they do not add significant information to a study in which measurements at given levels (instead of downhole trends) are compared. Furthermore, the GRAPE results from the deeper, rotary cored sections of the sites are not generally reliable because the measurements involve passing a gamma ray beam through the cores, and many of the core liners for the deeper cores are partially empty. It should be noted, however, that the GRAPE results from the hydraulic-piston-cored section may be extremely useful in future studies of the details of the variations of porosity and density in the softer sediments. Vane shear measurements were not made with the frequency of the other measurements, and we believe that the shear strength of the sediments should be studied in more detail before the existing data are presented.

[1] Mayer, L., Theyer, F., et al., *Init. Repts. DSDP*, 85: Washington (U.S. Govt. Printing Office).
[2] Addresses: (Wilkens) Massachusetts Institute of Technology, Cambridge, MA 02139; (Handyside) University of Newcastle-upon-Tyne, United Kingdom.

We did not make any corrections to the laboratory data to attempt to restore *in situ* conditions, although we realize that relationships for this purpose exist. We did not want to bias any of the measurements by correction factors that would not apply to every property. Thus, the data presented here were acquired at standard room temperature and pressure conditions.

SITE 574

We have discussed the downhole changes in physical properties in the Site 574 chapter (this volume) in some detail, but it is useful to review the data here before we look at the relationships among the various parameters. Figure 1 shows a plot of porosity, wet-bulk density, carbonate content, vertical formation factor, thermal conductivity, and compressional wave velocity versus depth for Site 574; the data for the upper 200 m are derived from HPC cores, and the data from 200 m to basement at approximately 520 m are derived from rotary cores. The measurements of formation factor and thermal conductivity were terminated at levels somewhat above basement because the probes used in making the measurements became unable to penetrate the sediments, which grew increasingly more competent as a result of lithification as depth increased.

The porosity and density plots, which essentially result from the same measurement, are mirror images of one another. Both properties are variable in the upper 100 m

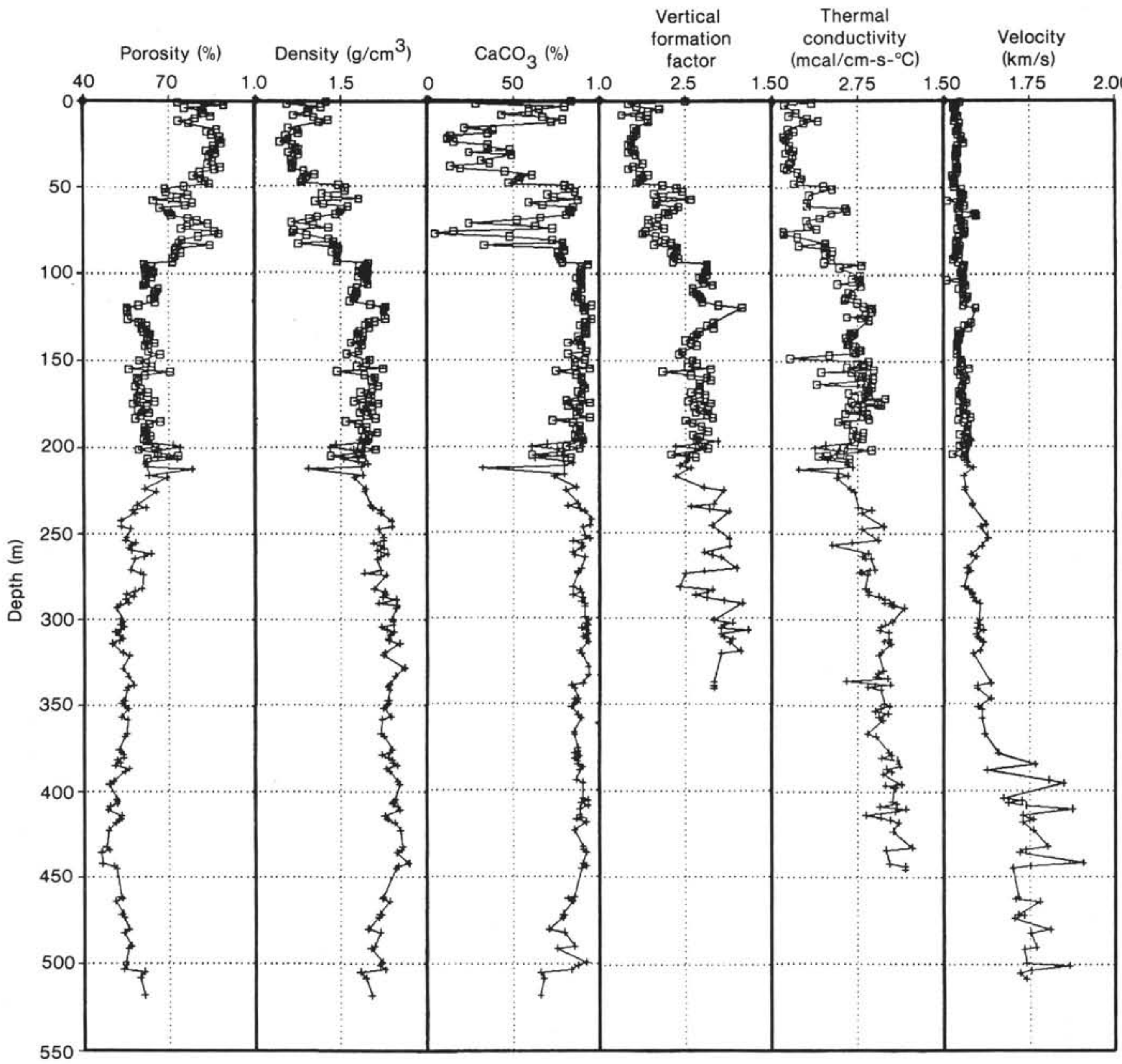

Figure 1. Depth plotted versus physical properties for Site 574. Data are from HPC Hole 574 (□) and rotary-cored Hole 574C (+). All measurements were made at room temperature and pressure.

of the sediment column and generally become more uniform with increasing depth. In some cases single points or groups of points show local maxima or minima within relatively constant sections. Especially in the case of the single points it is tempting to doubt the accuracy of the values and to attribute them to analytical error; however, these data are supported by independent measurements at the same level, such as carbonate content or thermal conductivity, and they represent true excursions in the profile.

Carbonate content is also extremely variable in the upper 100 m of sediment. It is included here with the physical properties because of the control of carbonate content on the porosity and density values, which are discussed in detail below. Most samples below a depth of 100 m had carbonate contents in excess of 80%, and almost all of the low-carbonate samples are from the unconsolidated ooze near the top of the section.

Both formation factor and thermal conductivity generally increase with increasing depth. They show the same general trends, and the changes correspond somewhat to the changes in wet-bulk density and porosity. Compressional wave velocity is the only property measured that does not appear to be variable over the shallow depth range. Velocities slowly increase with depth to about 380 m, where they exhibit a general increase and variability, in marked contrast to the smoothly varying values above 350 m.

Site 574 was piston cored twice to depths near 200 m to ensure the recovery of important biostratigraphic datums. To provide a check on the data, duplicate measurements were made on the second HPC core, although generally only two measurements were made per core rather than one per section (about one-third the number of measurements). Data from the two deep HPC holes at Site 574 are displayed in Figure 2, with an offset of the porosity values of Hole 574A by 25% to facilitate comparison. The values are in excellent agreement and could easily be taken for duplicate measurements on the same core instead of measurements on different cores from the same site. Another point of interest is the amount of detail that is lost by enlarging the sampling interval by a factor of 3. It is clear that data taken only once or twice per core can indicate only general trends in the data and that the sediment cannot be assumed to be uniform between data points.

Density and Porosity

The basic controls on wet-bulk density in marine sediments are porosity and grain density. In the central equatorial Pacific Ocean, almost all of the sediment grains are biogenic, and the average grain densities reflect a mixture of biogenic silica (ρ_g = 2.1 to 2.3 g/cm^3; Baas Becking and Moore, 1959) and biogenic calcite (ρ_g = 2.72 g/cm^3). A plot of wet-bulk density versus porosity for Site 574 is shown in Figure 3. Superimposed on the plot are calculated lines of constant grain density for ρ_g = 2.4, 2.6, and 2.8 g/cm^3. In general, wet-bulk density appears to decrease smoothly with increasing porosity.

Figure 3 also shows a more subtle trend: grain density tends to decrease as porosity increases. The grain densities of samples with porosity less than 75% are generally between 2.6 and 2.7 g/cm^3, whereas samples with porosity greater than 75% tend to have grain densities less than 2.6 g/cm^3. Mayer (1979, 1982) observed the same

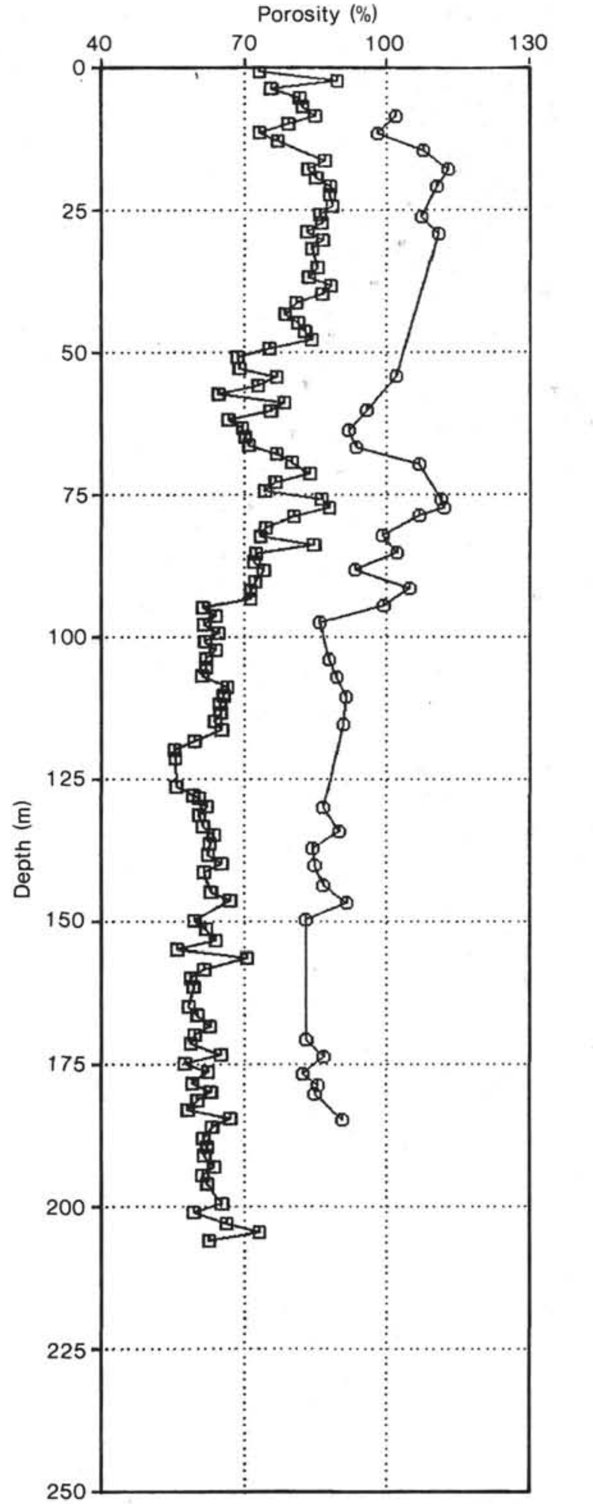

Figure 2. Depth plotted versus porosity for HPC Hole 574 (□) and Hole 574A (○). Values for Hole 574A are offset by +25% to facilitate comparison. All measurements were made at room temperature and pressure.

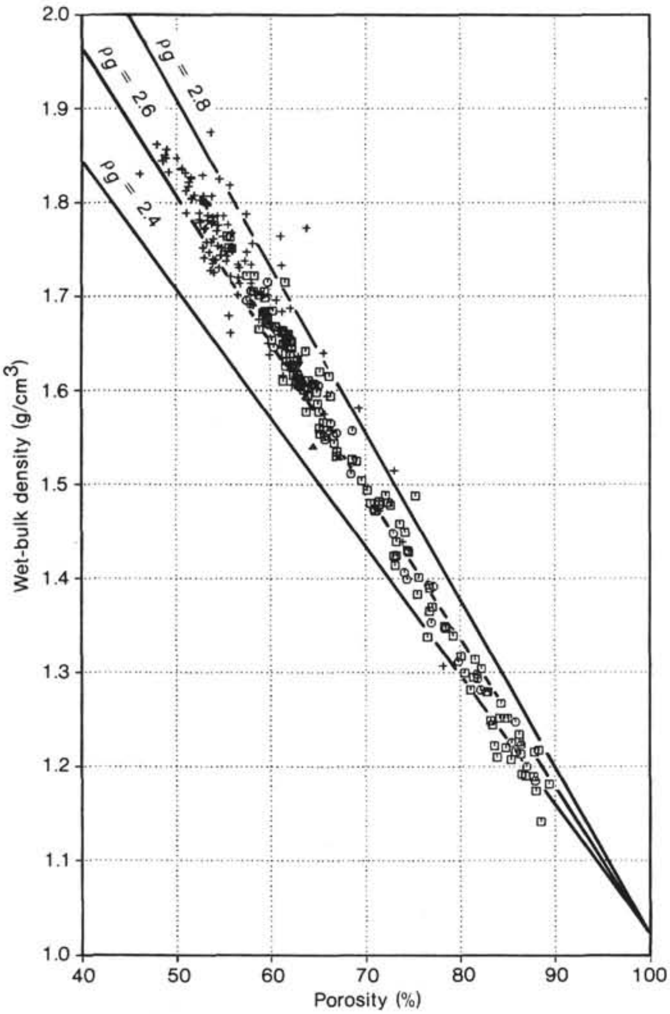

Figure 3. Wet-bulk density plotted versus porosity for Site 574. Data are from Holes 574 (□), 574A (○), 574B (△), and 574C (+). Lines are calculated relationships for constant grain density (ρ_g) of 2.4, 2.6, and 2.8 g/cm^3. All measurements were made at room temperature and pressure.

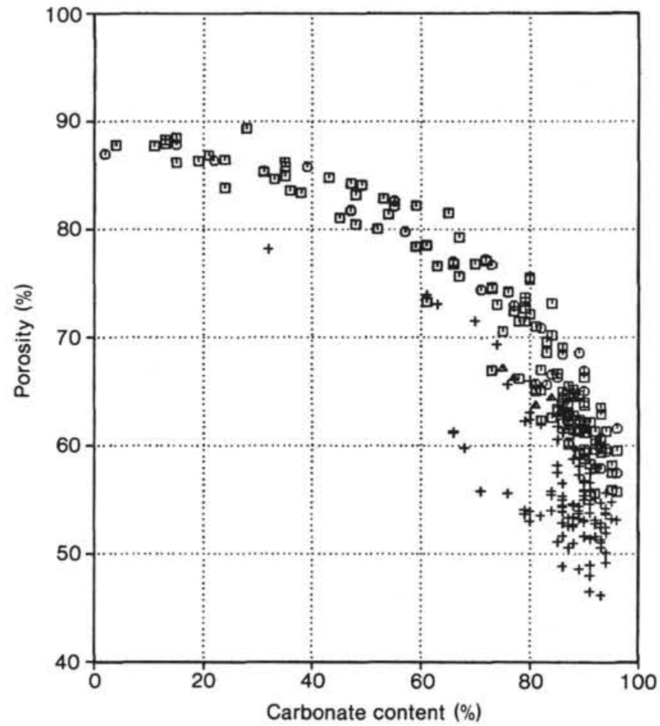

Figure 4. Porosity plotted versus carbonate content for Site 574. Symbols as in Figure 3. All measurements were made at room temperature and pressure.

trends in eastern equatorial Pacific sediments. Higher density sediments are composed predominantly of platy calcareous nannofossil tests, whereas lower density (higher porosity) samples contain a relatively greater amount of siliceous open-work radiolarian tests. These radiolarian tests lower the sediment density by both lowering the average grain density and keeping the framework of the sediment open as the result of the voids inside the grains.

The effect of carbonate content on porosity is illustrated in Figure 4, a plot of percent porosity versus percent carbonate. Sediments low in carbonate have the highest porosities, suggesting that the siliceous components of the sediments tend to hold the framework open. The effects of compaction are also apparent in the distribution of the data. For a given compositional range the samples from deeper in the sediment column have lower porosities (Hole 574C).

Velocity

The relationship between compressional wave velocity and porosity is shown in Figure 5. For values of porosity greater than approximately 60%, velocities remain fairly close to 1.55 km/s. These values reflect a fluid-dominated system of relatively unconsolidated sediment particles. Velocities increase dramatically as porosity decreases below about 55%, an effect of the onset of the lithification of the sediments. Gradually, as the sediment is buried, connective links form between sediment grains. The links substantially increase both the bulk modulus and the ridigity of the material, changes that in turn increase velocity. It is interesting that in sedimentary rocks on land, porosity is an important controlling factor in the value of compressional velocity (Wyllie et al., 1958), whereas in marine sediments velocity may remain relatively constant over a range of porosities or vary greatly within a limited porosity range.

The velocity-porosity relationship influences seismic stratigraphy, because the acoustic impedance of a sediment is the product of velocity and density, and in this case density and porosity are linearly related. Mayer (1979) showed that in soft sediments with relatively constant velocity it is density that controls acoustic impedance. Thus, the density contrasts in the upper sections of Site 574 (Fig. 1) will produce seismic reflections. In the lower part of the hole, however, the situation is reversed. Density and porosity remain relatively constant in comparison with velocity, which varies. The velocity variation is probably a response to the degree of lithification of any particular layer of sediment. Thus, at Site 574 the seismic reflectors near the surface (where increased carbonate deposition is correlated with increased density) may be the result of depositional environment, and the seismic reflectors near the basement (where increased lithi-

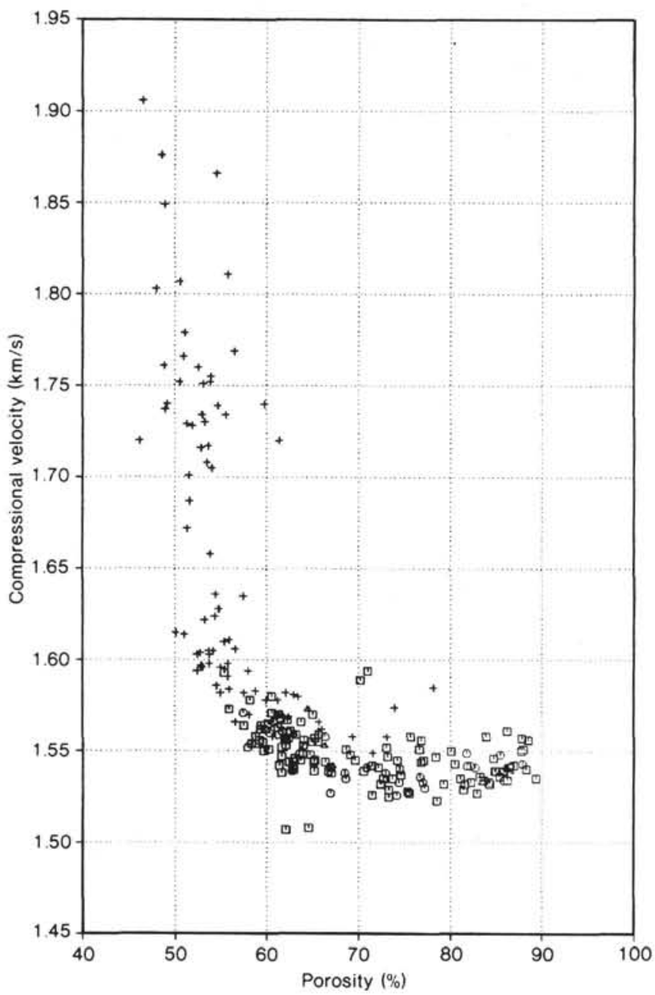

Figure 5. Compressional velocity plotted versus porosity for Site 574. Symbols as in Figure 3. All measurements were made at room temperature and pressure.

fication is correlated with increased velocity) may be the result of diagenetic state.

Thermal Conductivity and Formation Factor

Thermal conductivity and formation factor are measurements of the ability of the sediments to conduct heat and electricity, respectively. Because they are both conductive properties, it is not surprising that they have similar relationships to bulk sediment properties. A plot of thermal conductivity versus porosity is shown in Figure 6. The lines in the plot represent theoretical values of thermal conductivity that were calculated by using the weighted geometric mean equation of Woodside and Messmer (1961). This equation describes the conductivity of unconsolidated two-phase media with random distributions of the phases and has the form

$$K = K_f^{\varphi} K_s^{(1-\varphi)},$$

where K is the thermal conductivity, K_f is the fluid conductivity, K_s is the solid conductivity, and φ is the porosity, expressed as a fraction. The upper line in Figure 6

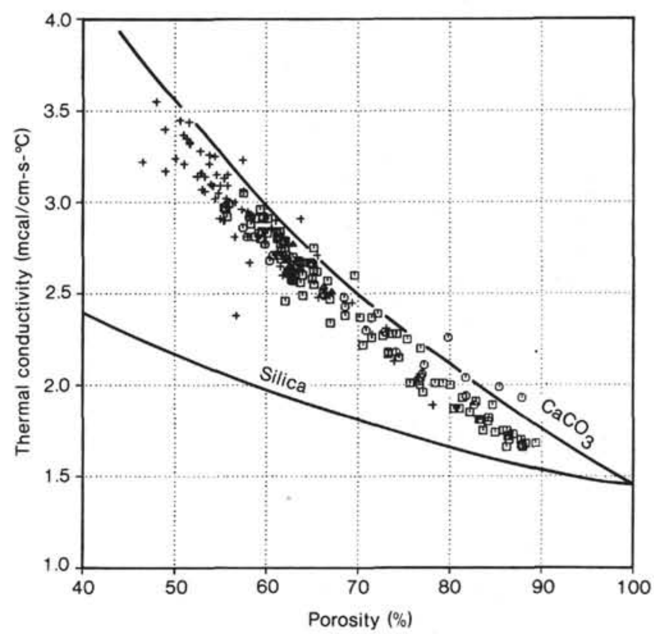

Figure 6. Thermal conductivity plotted versus porosity for Site 574. Symbols as in Figure 3. Lines are theoretical relationships of Woodside and Messmer (1961) for calcite and fused quartz. All measurements were made at room temperature and pressure.

represents a mixture of calcite and seawater (K_f = 1.46, K_s = 8.58 mcal/cm-s-C°; Horai and Simmons, 1969), and the lower line represents fused silica and seawater (K_s = 3.25 mcal/cm-s-°C). The measured values of thermal conductivity generally fall close to the curve calculated for a calcite–seawater mixture. As porosity increases, however, silica content increases, and as a result the data fall off the calcite line and approach the silica line.

Formation factor was measured both horizontally (with probes normal to the core axis) and vertically (with probes parallel to the core axis). The values of the vertical and horizontal measurements are plotted against one another in Figure 7, along with the line $x = y$. Two observations may be made about the distribution of the data: (1) formation factor measured vertically is uniformly greater than formation factor measured horizontally, and (2) the difference between the two measurements is larger in the deeper samples (those from Hole 574C). Both of these observations can be related to the pore geometry of the sediments. The platy calcareous nannofossils are aligned horizontally when they are deposited on the seafloor and produce an overlapping structure much like brickwork. Horizontal formation factor is measured in the plane of these layers, whereas vertical formation factor is measured normal to them. An overlapping structure of platy grains would tend to keep conductive seawater paths open within the plane of the layering but to close those paths normal to the layering. The contrast between the two directions becomes more pronounced as the lithification of the deeper samples proceeds; the overlapping grains bond at the grain-to-grain contacts and the overall porosity of the sediment decreases through compaction. The data suggest that

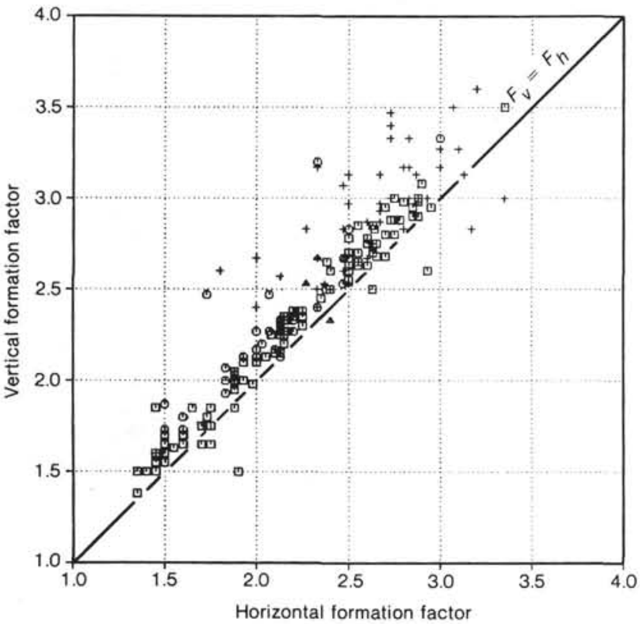

Figure 7. Vertical formation factor (F_v) plotted versus horizontal formation factor (F_h) for Site 574. Symbols as in Figure 3. Line is the relationship $F_v = F_h$. All measurements were made at room temperature and pressure.

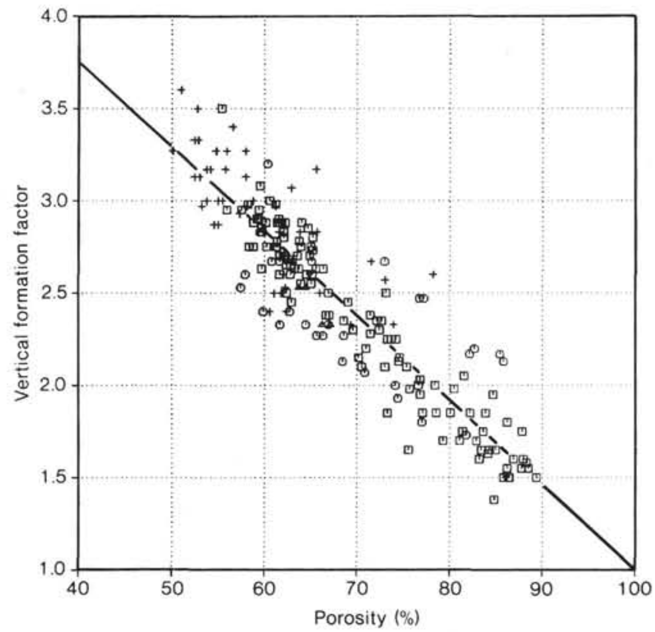

Figure 8. Vertical formation factor plotted versus porosity for Site 574. Symbols as in Figure 3. Line is linear least-squares fit to data; equation is given in text. All measurements were made at room temperature and pressure.

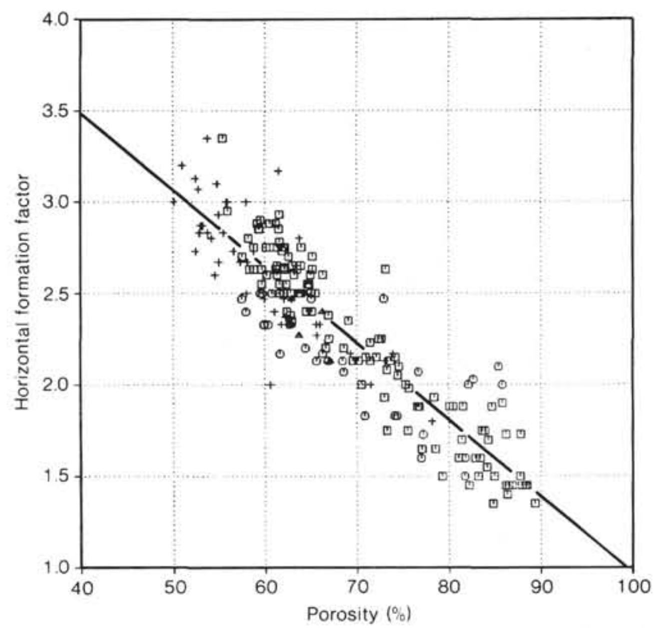

Figure 9. Horizontal formation factor plotted versus porosity for Site 574. Symbols as in Figure 3. Line is linear least-squares fit to data; equation is given in text. All measurements were made at room temperature and pressure.

the conductive paths in the plane of layering are kept open longer than those perpendicular to the plane of layering.

We display the relationship between the vertical and horizontal formation factor and porosity in Figures 8 and 9. Least-square regressions of the data have the form:

$$F_v = -0.0456\varphi + 5.5680,\ r^2 = 0.84,\ N = 195$$

$$F_h = -0.0421\varphi + 5.1679,\ r^2 = 0.84,\ N = 195$$

where F is formation factor, φ is porosity (%), r^2 is the coefficient of determination, and N is the number of measurements. Both data fields have similar distributions about their respective regression values. There is some indication that measurements of deep samples in the vertical sense depart slightly more than the horizontal values from their respective regression lines.

Because formation factor can be measured continuously *in situ* in a borehole by using electric logging techniques and thermal conductivity cannot, it is interesting to crosscorrelate the two properties to develop the empirical relationship between them. The relationship at Site 574 (Fig. 10) is as follows:

$$F_v = 0.772K + 0.577,\ r^2 = 0.82,\ N = 175.$$

While the scatter is not negligible, for most points the relationship holds to $\pm 10\%$, which is within the realm of combined error in the measurements themselves. Moreover, an examination of the pore structure and mineralogy of the sediments at different levels might explain why some data deviate from the regression equation values.

INTERSITE COMPARISONS

Of the data available, we elected to compare the porosity and compressional velocity data for Sites 572 to 575. The relationships between porosity and density, formation factor, and thermal conductivity are generally lin-

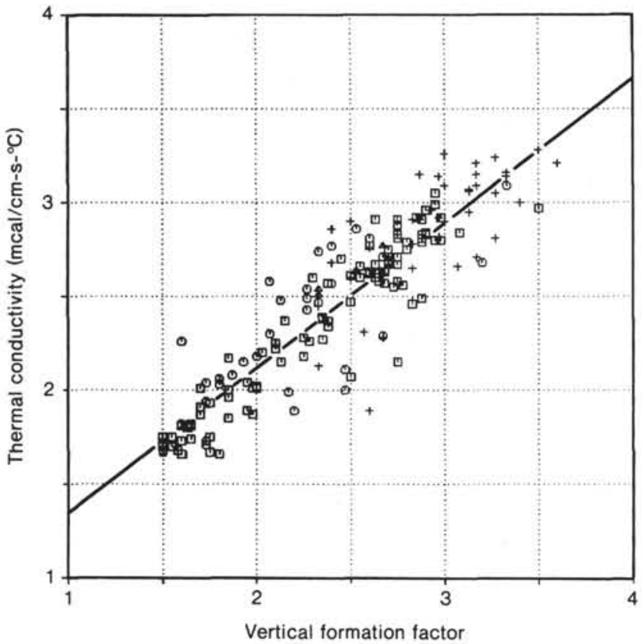

Figure 10. Thermal conductivity plotted versus vertical formation factor for Site 574. Symbols as in Figure 3. Line is linear least-squares fit to data; equation is given in text. All measurements were made at room temperature and pressure.

ear, so intersite comparisons of all these properties would tend to mimic one another. As demonstrated above, velocity is not simply related to porosity and therefore deserves separate analysis. As discussed above, these two factors also affect the acoustic impedance and therefore the acoustic stratigraphy of the sediments. We first examine the changes in each of these properties with increasing depth at each site and then, by using the sedimentation rates from the site chapters to convert the depth data to age data, examine how these properties changed at each site over time.

Depth

Porosity and velocity data for Sites 572 to 575 are plotted versus depth in Figures 11 and 12, respectively. The drilling at Site 575 did not reach basement (which was estimated from seismic survey data to be at a depth of approximately 500 m), so the data for that site do not reflect the entire sedimentary column. The sites do appear to have some characteristics in common.

There is a general variability of porosity in the uppermost 100 m or so of sediment. The values tend to decrease with depth, although the rate of decrease varies from site to site. The porosities of the near-surface sediments are around 80% at all of the sites, and the Site 572 values remain near 70% to depths in excess of 400 m. At the other sites the porosity values are less than 70% at depths greater than 175 m. Thus, mechanical loading operates differently on the porosity of the sediment column at Site 572 than at the other sites. Sites 573 and 574 are predominantly calcareous at greater depths, but the silica content remains between 30 and 40% for much of the Site 572 sediment column, so the radiolarian tests may increase porosity by holding the sediment framework open.

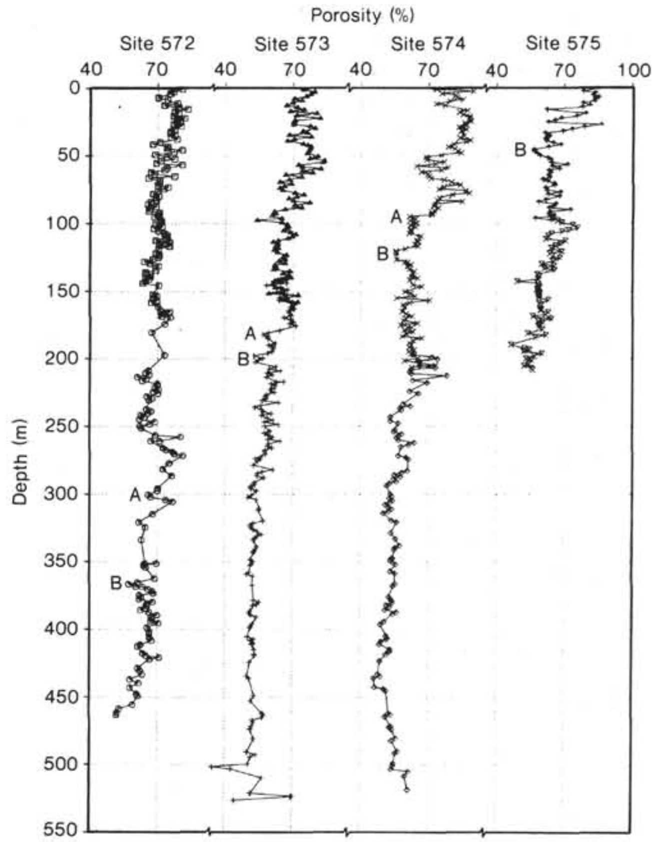

Figure 11. Depth plotted versus porosity for Sites 572, 573, 574, and 575. Data are from Holes 572C (□), 572D (○), 573 (△), 573B (+), 574 (×), 574C (◇), 575 (↑), 575A (⌧). Letters A and B represent events of similar age discussed in text. All measurements were made at room temperature and pressure.

The change in velocity with increasing depth (Fig. 12) is very similar at all four sites: velocity increases very gradually for most of the sections. Abrupt changes in velocity take place that are attributed to increasing lithification, but they do not occur at the same level at each site. At Sites 572 and 573 the change takes place somewhere within 50 m of basement, whereas at Site 574 the change takes place well over 100 m above basement.

Age

We used the sedimentation rates derived from the biostratigraphy at each site to convert the depth of each measurement into an age. Age data are as given in the site chapters and the introduction to the volume and are not adjusted to later data as given in Barron et al. (this volume). Porosity values versus age for the four sites are plotted in Figure 13. We have only displayed the data for the past 25 m.y. because only two of the four sites reached sediment older than that age. Because our sampling was carried out at regular depth intervals, the spacing of the data with respect to time is controlled by sedimentation rate. Thus, in the upper sections of Sites 572 and 573 the data are closely spaced, reflecting the present position of the sites in the equatorial high-productivity zone. Sites 574 and 575 have moved north out of the axis of high productivity. Their uppermost sections show longer time intervals between samples as the result of

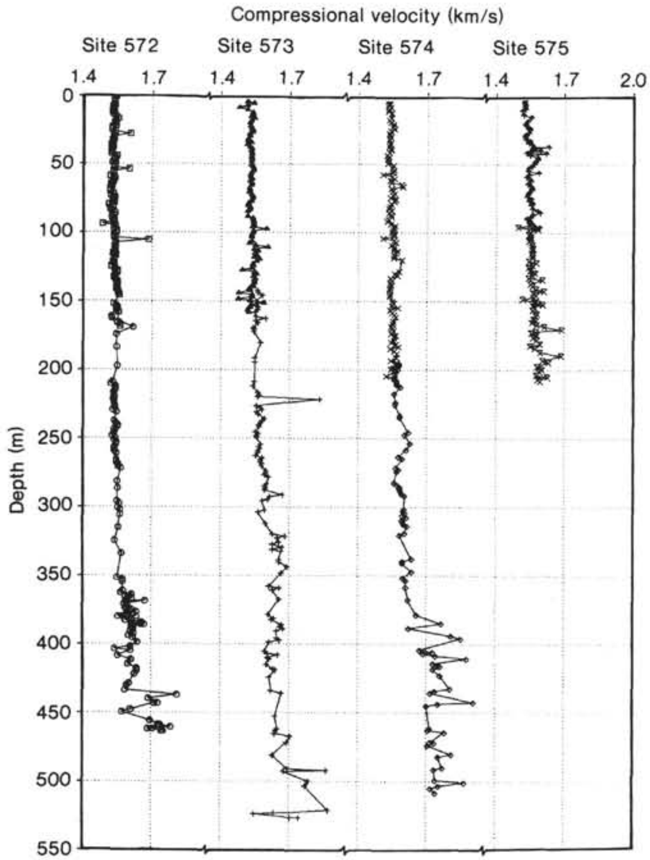

Figure 12. Depth plotted versus velocity for Sites 572, 573, 574, and 575. Symbols as in Figure 11. All measurements were made at room temperature and pressure.

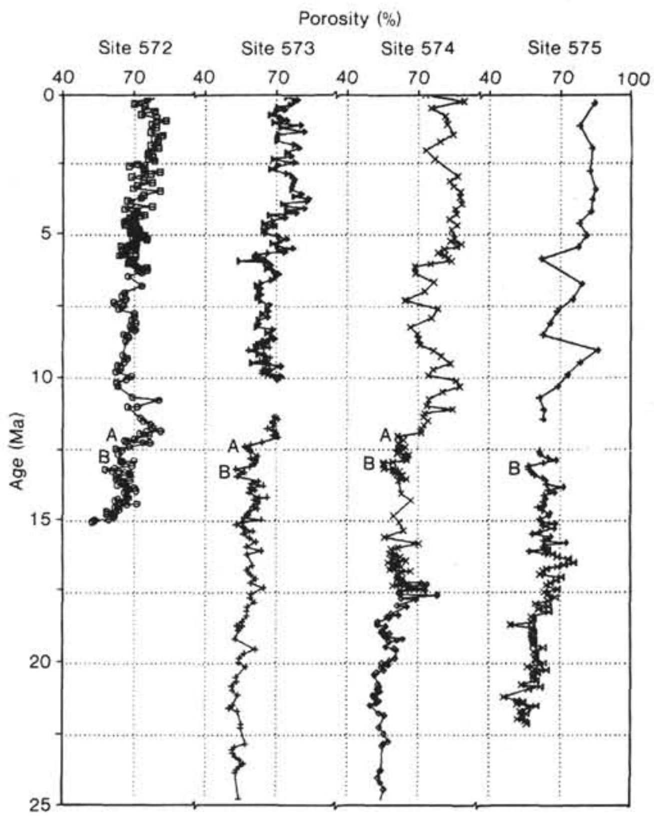

Figure 13. Age plotted versus porosity for Sites 572, 573, 574, and 575. Symbols as in Figure 11. Letters A and B represent events of similar age discussed in text. All measurements were made at room temperature and pressure.

the lower sedimentation rate, although deeper in the sections the data density increases, indicating the time in the past when these sites were within the high-productivity zone. Gaps between 10 and 12.5 Ma Sites 573 and 575 are hiatuses or perhaps erosional events not seen at the other sites.

An examination of velocity versus age (Fig. 14) shows that sediments younger than 25 Ma that have undergone sufficient lithification to enhance compressional velocity occur only at Site 572. The change in lithification occurs at Site 573 at about 490 m depth, which is equivalent to about 38 Ma, while that at Site 574 occurs at 380 m, which is equivalent to about 28 Ma. The age of lithification is different at each site, and, more important, except at the very bottom of Site 572 the sediments younger than 25 Ma show only the generally uniform, gradual rise in velocity with age reflected in the velocity-depth relationships.

In the time frame considered, porosity (density) controls the seismic reflection profile. Thus, at the levels at which abrupt changes in porosity occur that can be correlated between sites we would expect to find time-equivalent reflectors. An example of such a change occurs at around 12 to 13 Ma (Fig. 13). Sites 572, 573, and 574 all show decreases in porosity at around 12 Ma; then all four sites have another decrease near 13 Ma. We call the 12-Ma event A and the 13-Ma event B and have indicated their position in the actual sediment column in Figure 11. Event A occurs at depths of a little over 300 m at Site 572, at 175 m at 573, at 90 m at 574, and is not present as the result of a hiatus or erosional episode at Site 575. Event B is at a depth of 365 m at Site 572, 190 m at 573, 120 m at 574, and 40 m at Site 575.

It is beyond the scope of this study to explain these sets of correlatable changes in sediment properties. Rather, we point out that these two events, and several others, are probably responsible for continuous or nearly continuous reflectors that reach from site to site in the seismic survey data (see also Mayer et al., this volume). In view of the nature of the interval, they appear to define some environmental event that affected carbonate production and through it the eventual degree of sediment porosity. We also see events that may be more local in nature; that is, they affect Sites 573 to 575 but are absent 1000 km to the east at Site 572. An examination of the sediments deposited during these events, in combination with an indication of their extent from seismic reflections, should provide new information about paleoceanographic change in equatorial Pacific sedimentation.

ACKNOWLEDGMENTS

The authors would like to thank B. Charlotte Schreiber, Marcus Langseth, and N. Christensen for their reviews of this paper. It has benefited greatly from their comments.

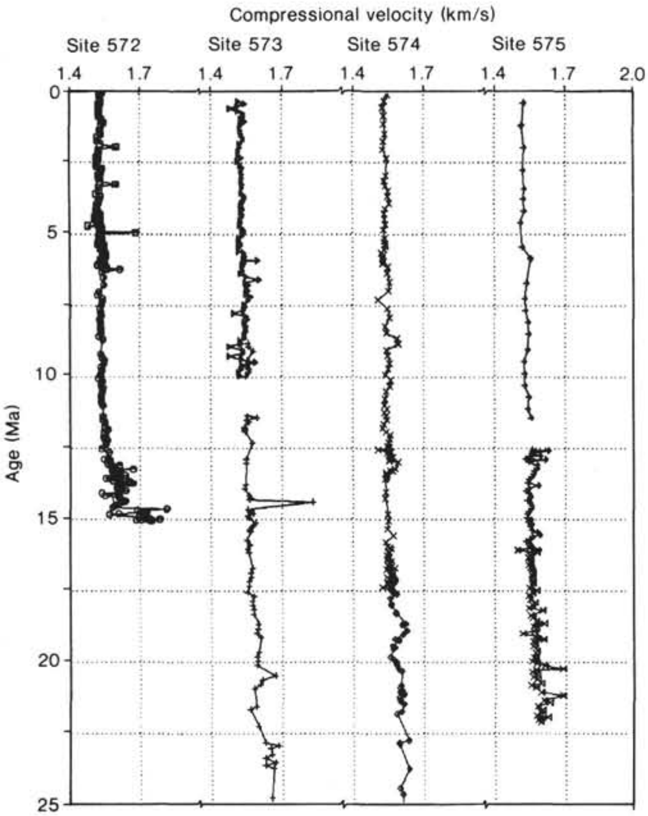

Figure 14. Age plotted versus compressional wave velocity for Sites 572, 573, 574, and 575. Symbols as in Figure 11. All measurements were made at room temperature and pressure.

REFERENCES

Baas Becking, L. G. M., and Moore, D., 1959. Density distribution in sediments. *J. Sediment. Petrol.*, 29:45-55.

Boyce, R. E., 1976. Definitions and laboratory techniques of compressional sound velocity parameters and wet-water content, wet-bulk density, and porosity parameters by gravimetric and gamma ray attenuation techniques. *In* Schlanger, S. O., Jackson, E. D., et al., *Init. Repts. DSDP*, 33: Washington (U.S. Govt. Printing Office), 931-958.

_______, 1977. Deep Sea Drilling Project procedures for shear strength measurement of clayey sediment using modified Wykeham Farrance Laboratory vane apparatus. *In* Barker, P. F., Dalziel, I. W. D., et al., *Init. Repts. DSDP*, 36: Washington (U.S. Govt. Printing Office), 1059-1068.

Horai, K., and Simmons, G., 1969. Thermal conductivity of rock forming minerals. *Earth Planet. Sci. Lett.*, 6:359-368.

Manheim, F. T., and Waterman, L. S., 1974. Diffusimetry (diffusion constant estimation) on sediment cores by resistivity probe. *In* von der Borch, C. C., Sclater, J. G., et al., *Init. Repts. DSDP*, 22: Washington (U.S. Govt. Printing Office), 663-670.

Mayer, L. A., 1979. Deep sea carbonates: acoustical, physical, and stratigraphic properties. *J. Sediment. Petrol.*, 49:819-836.

_______, 1982. Physical properties of sediment recovered on Deep Sea Drilling Project Leg 68 with the hydraulic piston corer. *In* Prell, W. L., Gardner, J. V., et al., *Init. Repts. DSDP*, 68: Washington (U.S. Govt. Printing Office), 365-382.

Von Herzen, R. P., and Maxwell, A. E., 1959. The measurement of thermal conductivity of deep-sea sediments by a needle probe method. *J. Geophys. Res.*, 64:1557-1563.

Woodside, W., and Messmer, J. H., 1961. Thermal conductivity of porous media. I. Unconsolidated sediments. *J. Appl. Phys.*, 32: 1688-1699.

Wyllie, M. R. J., Gregory, A. R., and Gardner, G. H. F., 1958. An experimental investigation of factors affecting elastic wave velocities in porous media. *Geophysics*, 23:459-493.

Date of Initial Receipt: 3 November 1984
Date of Acceptance: 22 April 1984